Quarkonium Spectroscopy in the Quark-Gluon Plasma

Zhanduo Tang¹, Biaogang Wu¹, Andrew Hanlon², Swagato Mukherjee³, Peter Petreczky³, and Ralf Rapp¹

¹Cyclotron Institute and Department of Physics and Astronomy, Texas A&M University, College Station, TX 77843-3366, U.S.A. ²Department of Physics, Kent State University, Kent, OH 44242, U.S.A. ³Physics Department, Brookhaven National Laboratory, Upton, NY 11973, U.S.A. (Dated: February 14, 2025)

The properties of bound states are fundamental to hadronic spectroscopy and play a central role in the transition from hadronic matter to a quark-gluon plasma (QGP). In a strongly coupled QGP (sQGP), the interplay of temperature, binding energy and large collisional widths of the partons poses formidable challenges in evaluating the in-medium properties of hadronic states and their eventual melting. In particular, the existence of heavy quarkonia in the QGP is a longstanding problem that is hard to solve by considering their spectral properties on the real-energy axis. We address this problem by analyzing in-medium thermodynamic quarkonium T-matrices in the complex energy plane. We first validate this method in vacuum, where the T-matrix poles of observed states are readily identified. When deploying this approach to recent self-consistently calculated T-matrices in the QGP, we find that poles in the complex energy plane can persist to surprisingly large temperatures, depending on the strength of the in-medium interactions. While the masses and widths of the pole positions are precisely defined, the notion of a binding energy is not due to the absence of thresholds caused by the (large) widths of the underlying anti-/quark spectral functions. Our method thus provides a new and rigorous quantum-mechanical criterion to determine the melting temperature of hadronic states in the sQGP while increasing the accuracy in the theoretical determination of transport parameters.

PACS numbers:

Introduction.— The search and characterization of phase transitions in Quantum Chromodynamics (QCD) matter is at the forefront of contemporary research. The changes in the properties of hadrons as the strongly interacting medium transits from confined and chirally broken hadronic matter into a deconfined and chirally restored quark-gluon plasma (QGP) play a pivotal role in this endeavor. While ultrarelativistic heavy-ion collisions (URHICs) have provided ample evidence for the formation of a QGP [1, 2], a microscopic description of its properties based on the underlying QCD forces remains a key challenge. Heavy quarkonia have been realized early on as a prime probe of the deconfinement transition [3], due to their sensitivity to the "confining force" in the heavy-quark (HQ) potential that is by now well established in the vacuum [4, 5]. The original idea of a suppression of quarkonia due to Debye screening has developed into a more complex picture which requires kinetic transport approaches based on inelastic reaction rates [6]. The interplay of the reaction rates, representing the quarkonium decay widths, with the (in-medium) binding energies of the various quarkonium states is expected to govern their melting in the medium. At the same time, regeneration reaction will commence once the cooling medium in the expanding fireball supports the reformation of the bound states. The notion of a "melting temperature", which is of both practical and principal importance, plays a key role in this context. Various prescriptions to define it have been proposed in the literature, e.g., the vanishing of the in-medium binding energy

or the latter becoming comparable to the dissociation width, but a precise criterion has not been identified to date, cf. Refs. [7-11] for reviews. All previous studies of quarkonia in the QGP were, in fact, restricted to the realenergy axis. But even in quantitative studies of spectral functions which treat binding energies and dissociation rates on the same footing, one is usually limited to the analysis of peak structures which are well defined only as long as their width remains reasonably small. However, as temperatures rise, the peaks became broader, which is further complicated as the bound state loses binding energy and merges in the continuum. For resonances the notion of a binding energy becomes rather meaningless. In Refs. [12, 13] the concept of Jost functions was deployed to identify bound states via a zero in the real part of the determinant of the scattering amplitude, signaling the presence of a pole. However, also these analyses, designed for narrow bound states, remain inconclusive, especially if large imaginary parts driven by high HQ scattering rates in the QGP render the zero crossings quite shallow and do not render a true pole.

In this paper, we propose a resolution to this issue by performing a complex-pole analysis of in-medium $Q\bar{Q}$ scattering amplitudes in the QGP. Specifically, we will be able to unambiguously identify the presence of a quarkonium state by a pertinent pole in the complex energy plane. This method is well known in the analysis of bound-state structures in the vacuum [14–16], especially in multi-channel problems where the presence of thresholds leads to finite decay widths and thus shifts

the location of bound-state poles into the complex plane. An in-medium T-matrix analysis has been conducted in Ref. [17] for the $D\bar{D}^*$ loop of a dynamically generated X(3872) particle, by using a constant effective (complex) mass for the D-meson selfenergies. Here, we will introduce a method where the full off-shell properties of the single-particle propagators are accounted for, which is particularly important in a strongly coupled medium with large collision widths. We will then deploy this method to carry out quantitative analyses of bottomonium states for two scenarios: (i) strongly coupled scenario where the HQ potential is large and the collisional rates of the heavy quarks are high, and (ii) a relatively weakly coupled QGP with a substantially screened HQ potential and small collision rates. The main vehicle, well suited for our objective, is the thermodynamic T-matrix approach, which has been developed in recent years to establish a microscopic description of heavy quarks and quarkonia that is selfconsistently embedded into a sQGP.

Quantum Many-Body Approach. – Let us first recall the basic ingredients and results of the thermodynamic T-matrix formalism. It is based on a coupled set of 1- and 2-body correlation functions (propagators and scattering amplitudes) for heavy quarks (Q) and antiquarks (\bar{Q}) and their interactions in the QGP, schematically given by [12, 18, 19]:

$$T_{Q\bar{Q}}(E, p, p') = V_{Q\bar{Q}}(p, p') + \int d^3k V_{Q\bar{Q}}(p, k) \times G_{Q\bar{Q}}(E, k) T_{Q\bar{Q}}(E, k, p'), \tag{1}$$

$$G_{Q\bar{Q}}(E,k) = \int dk_0 G_Q(E-k_0,k) G_{\bar{Q}}(k_0,k),$$
 (2)

$$G_Q(k_0, k) = 1/[k_0 - \varepsilon_Q(k) - \Sigma_Q(k_0, k)],$$
 (3)

$$\Sigma_Q(k_0, k) = \int d^4p T_{Qi}(k_0 + p_0, k, p) G_i(p_0, p) n_i$$
 (4)

where $T_{Q\bar{Q}}$ is the quarkonium T-matrix, $G_{Q,i}$ are the single-parton propagators for heavy quarks (Q) or thermal light partons $(i=q,\bar{q},g)$, and $G_{Q\bar{Q}}$ denotes the 2-body propagator as a convolution over the HQ propagators. The on-shell energies, $\varepsilon_{Q,i} = \sqrt{M_{Q,i}^2 + k^2}$, include in-medium particle masses $M_{Q,i}$ and energy-momentum dependent selfenergies, $\Sigma_{Q,i}$, which are computed self-consistently from the pertinent in-medium T-matrices. The kernel of the T-matrix, $V_{Q\bar{Q}}$, is an input quantity constrained by lattice QCD (lQCD). In the color-singlet we make the ansatz [20]

$$\widetilde{V}(r,T) = -\frac{4}{3}\alpha_s \left[\frac{e^{-m_d r}}{r} + m_d \right] - \frac{\sigma}{m_s} \left[e^{-m_s r - (c_b m_s r)^2} - 1 \right]$$
(5)

which in vacuum reduces to the well-known Cornell potential, $\widetilde{V}(r) = -\frac{4}{3}\frac{\alpha_s}{r} + \sigma r$, where $\alpha_s = 0.27$ and $\sigma = 0.225 \text{ GeV}^2$ are chosen to reproduce the vacuum free energy from lQCD [21]. The parameters m_d and

 m_s represent the Debye screening masses for the shortrange color-Coulomb and long-range string interactions. respectively, and the parameter c_b simulates in-medium string breaking at large distances. Upon Fourier transforming to momentum space, relativistic corrections [18] are included which also feature a vector component in the confining potential to better fit the empirical spininduced splittings of charmonia and bottomonia in vacuum [22]. We furthermore account for what has been referred to as an imaginary part of the potential [23], which results from an interference of inelastic parton scattering off the Q and \bar{Q} within the quarkonium state. This suppresses the dissociation width with decreasing radius until it vanishes for $r \to 0$ (colorless limit). Diagramatically, it corresponds to 3-body effects which, for simplicity, have been parameterized by a perturbatively inspired interference function [19, 23, 24].

In our numerical results shown below we utilize the recently evaluated constraints based on lQCD "data" for HQ free energies and Euclidean correlation functions [19], as well as static Wilson line correlators (WLCs) [24]; within each scenario the in-medium interactions and spectral functions in the sQGP are computed with the same kernel and constrained by the QGP equation of state (EoS) [19]. The WLC constraints require an input potential which requires little Debye screening at small QGP temperatures, leading to large collisional widths for both light and heavy partons, in excess of 0.5 GeV at all temperatures considered. This, in turn, produces transport parameters which are in the range required by heavy-ion phenomenology. On the other hand, we also employ a "weakly coupled scenario" (WCS) which is compatible with constraints from HQ free energies and euclidean correlators; in this scenario, the screening is much stronger requiring a much weaker in-medium potential. The differences in these two scenarios will serve to illustrate the pertinent consequences for the in-medium spectroscopy of quarkonia.

T-matrix at Complex Energies.— We are now in position to discuss our T-matrix analysis in the complex energy plane, thereby focusing on the case of bottomonia, as this system provides the largest mass scale ($m_b \simeq 5 \text{ GeV}$). We first observe that the energy (E) dependence of the T-matrix, Eq.(1), is generated entirely by the 2-body propagator. In the limit of small widths one can carry out the energy integration to obtain

$$G^0_{b\bar{b}}(E,k) = \frac{1}{E \pm i\epsilon - 2\varepsilon_b(k)},\tag{6}$$

where the $+i\epsilon$ case corresponds to the standard physical sheet (first Riemann sheet) with $\mathrm{Im}G_{b\bar{b}}<0$, while the $-i\epsilon$ case is usually referred to as the second Riemann sheet, which contains the information on bound states [25, 26]. To access this information in the QGP, we define a (complex) 2-body selfenergy, $\Sigma_{b\bar{b}}(E,k)$, from

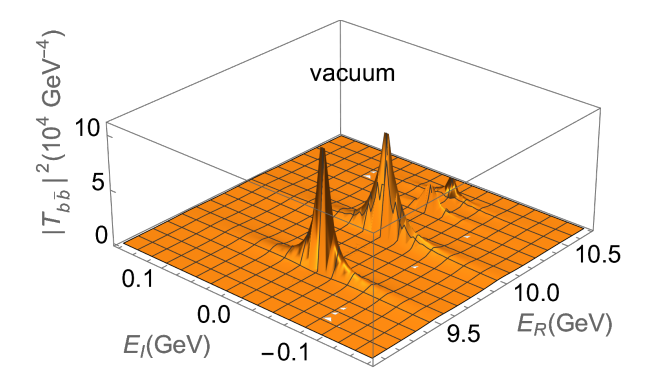


FIG. 1: The S-wave bottomonium T-matrix as functions of the real (E_R) and imaginary (E_I) energies at zero center-of-mass momentum in vacuum. For illustration purposes a small (artificial) b-quark width of 20 MeV has been introduced in the 2-body propagator. All Υ states are below the vacuum $b\bar{b}$ threshold of 10.513 GeV.

the in-medium propagator in Eq. (2) via [19]

$$G_{b\bar{b}}^{0}(E,k) = \frac{1}{E - 2\varepsilon_{b}(k) - \Sigma_{b\bar{b}}(E,k)} . \tag{7}$$

We then extend this expression into the complex energy plane, i.e., $E \to z = E_R - iE_I$ with $E_I > 0$, by

$$G_{b\bar{b}}^{0}(z,k) = \frac{1}{z - 2\varepsilon_{b}(k) - \Sigma_{b\bar{b}}(E_{R},k)} . \tag{8}$$

For $E_I \to 0$ we recover the usual second Riemann sheet in the complex plane, and by restricting the energy argument of the two-body selfenergy to its real part, we ensure that the former reflects the physical properties of the $Q\bar{Q}$ states. In essence, the imaginary part of z serves as a "probe" of the imaginary part of the selfenergy. To illustrate this more explicitly, we can write the solution of the T-matrix equation in operator form as

$$T(z) = \frac{V}{1 - G_2(z)V}$$
, (9)

where the denominator is referred to as "T-matrix determinant" or Jost function. Its real part corresponds to a "gap equation", which develops a zero if the potential is strong enough; large imaginary parts in the selfenergy of the 2-body propagator, G_2 , tend to suppress possible solutions. On the other hand, for the imaginary part of the determinant to vanish, the imaginary part of z has to compensate the value of $\text{Im}\Sigma_{b\bar{b}} < 0$. A pole of T(z) signals a quarkonium state thereby quantifying its mass and width, $\Gamma_Y = 2E_I^{\text{pole}}$. In the following we utilize this method to examine the pole structure of bottomonia from selfconsistent in-medium T-matrix calculations for the two different input potentials as described above.

Before conducting the finite-temperature analysis, we benchmark our procedure by investigating the vacuum T-matrix, calculating its absolute values squared in the

complex energy plane, cf. Fig. 1 for S-wave states. To better visualize the results, we adopt a small $b\bar{b}$ selfenergy of $\mathrm{Im}\Sigma_{b\bar{b}}{=}-20$ MeV in the propagator, shifting the bound-state positions to $E_I=-20$ MeV and generating peak widths of $-2\mathrm{Im}\Sigma_{b\bar{b}}=40$ MeV. We recover our previously identified $\Upsilon(1S), \Upsilon(2S), \Upsilon(3S)$. In addition, we can identify the $\Upsilon(4S)$, which is located very close to the vacuum $b\bar{b}$ threshold and was not discernible from the real axis of the spectral functions in our earlier work [22].

Bottomonium Spectroscopy in the QGP.— We start with the in-medium T-matrices resulting from a potential that has recently been constrained by lQCD data from Wilson-line correlators [24]. The main feature of this potential is a weak screening even at relatively large temperatures. The absolute values squared of the T-matrices are displayed in the complex energy plane in Fig. 2. At the lowest temperature considered, $T=195\,\mathrm{MeV}$, one clearly recognizes the 3 poles corresponding to the $\Upsilon(1S)$, $\Upsilon(2S)$ and $\Upsilon(3S)$. In the QGP, the $b\bar{b}$ threshold, $2m_b(T)$, is no longer well defined due to the large widths of the underlying b-quark spectral function. However, to make a qualitative assessment of the states' "binding energy" (which is no longer well defined either), we adopt an operational definition of a "nominal" $b\bar{b}$ threshold by using an effective mass of b-quarks as the average over their spectral function at each temperature. With this caveat, we find that at $T=195\,\mathrm{MeV}$, the $\Upsilon(1S)$ and $\Upsilon(2S)$ are still bound, with nominal binding energies (much) larger than their dissociation widths. However, for the $\Upsilon(3S)$, its width of $\sim 0.35\,\mathrm{GeV}$ is already well above its nominal binding energy of below 0.1 GeV. Even more surprising, the $\Upsilon(4S)$ still persists as a state above the nominal $b\bar{b}$ threshold, with a large width of $\sim 0.6 \,\text{GeV}$. These features suggest that there is no principal difference between a bound and resonance state in the OGP, while a state can still be unambiguously identified in the complex plane with a precisely defined mass and width. When increasing the temperature, the $\Upsilon(4S)$ vanishes at $T \simeq 250 \,\mathrm{MeV}$, with the $\Upsilon(3S)$ following suit at $T \simeq 330 \,\mathrm{MeV}$, see Fig. 3 for tracing the vanishing of its T-matrix determinant. The $\Upsilon(2S)$ survives up to $T \approx 700 \,\mathrm{MeV}$, while the $\Upsilon(1S)$ still persists to higher temperatures.

To put the melting temperatures extracted from our pole analysis into context with previously used schematic criteria based on nominal binding energies and dissociation widths, we summarize their temperature dependence in Fig. 4. Much higher melting temperatures are obtained from the pole analysis compared to previous estimates. In how far these features are related to recent lattice-QCD studies [27], where the use of extended-

¹ We note that this deviates from the standard nomenclature in vacuum spectroscopy [15, 16] where *any* state above the lowest mass threshold is referred to as "resonance".

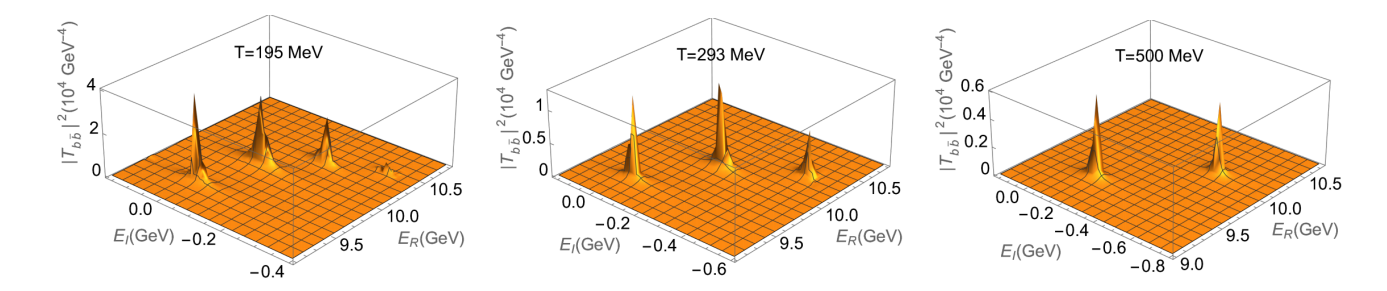


FIG. 2: The S-wave bottomonium T-matrices as functions of the real (E_R) and imaginary (E_I) energies at zero center-of-mass momentum at various temperatures for a strong potential constrained by WLCs, as following from our extension of the 2. Riemann sheet to finite temperature.

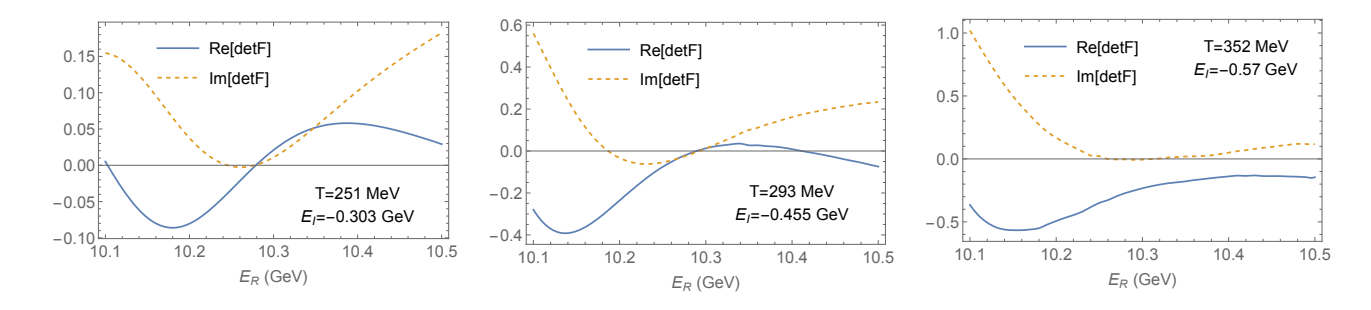


FIG. 3: Real and imaginary parts of Jost functions for the $\Upsilon(3S)$ vs. E_R at fixed E_I based on Fig. 2, illustrating its melting at $T \simeq 330 \,\mathrm{MeV}$.

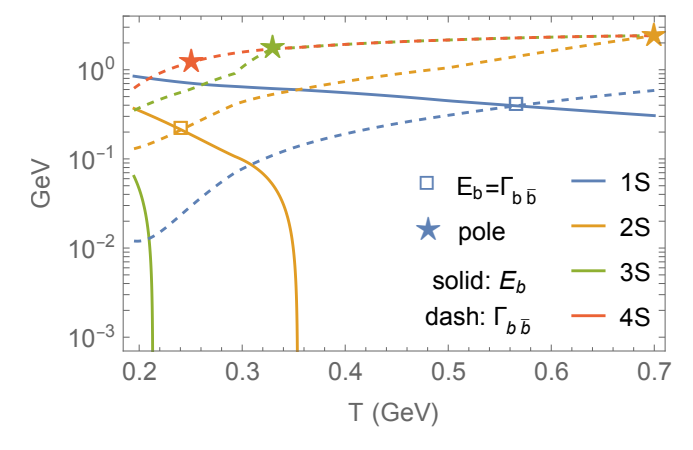


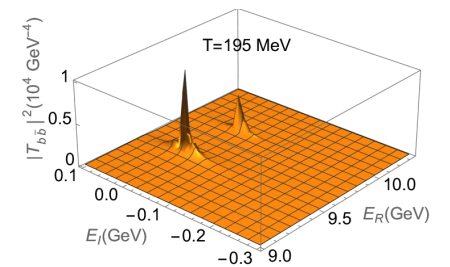
FIG. 4: Illustration of different melting criteria for S-wave bottomonia in the QGP. Solid line and dashed lines: nominal "binding energies" (see text) and decay widths, respectively, extracted from the T-matrix poles with WLC constraints; stars indicate the vanishing of the pole and open boxes the temperature where the width equals the binding energy.

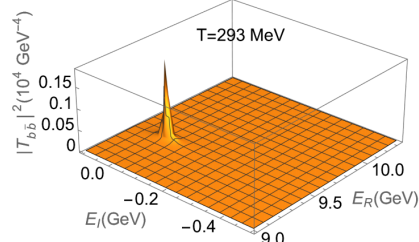
meson operators tailored to the spatial size of the vacuum states leads to rather well-defined peaks in pertinent spectral functions at relatively large temperatures, remains to be understood.

To highlight the role of the interaction potential in the QGP we show in Fig. 5 the results for S-wave bottomonium T-matrices in a "weakly coupled scenario" con-

strained by the HQ free energy [19]. The much stronger screening of the underlying potential translates into a much reduced binding, while at the same time the collisional parton widths are smaller by up to a factor of \sim 5 than those emerging from the WLC constraints. Consequently, only the 1S and 2S states are visible at the lowest temperature, while at higher temperatures solely the ground state survives, albeit with much reduced dissociation widths compared to the WLC constrained scenario. For this potential, states with vanishing nominal binding energies are not supported, suggesting that the latter are a characteristic of strong coupling.

Summary. - We have proposed a novel analysis to investigate "bound-state" properties in medium by analyzing pertinent two-body T-matrices in the complex energy plane. By extending the energy variable in a suitably defined two-body propagator in a way that retains the full-off-shell properties of the in-medium 1-body propagators, we are able to identify the in-medium poles of quark-antiquark states. This, in particular, allowed us to address the long-standing problem of the survival of quarkonia in the QGP, providing a rigorous criterion for their existence and melting temperatures, while quantifying their masses and dissociation widths. Concretely, we have applied this method within the self-consistent T-matrix approach to the QGP, to assess the fate of the bottomonium spectrum in partonic matter. By testing two scenarios, roughly corresponding to a strongly





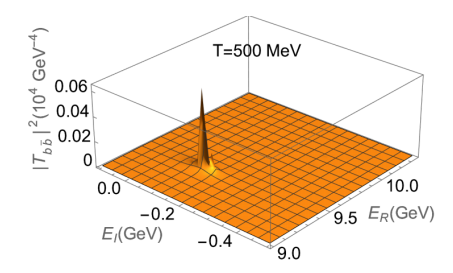


FIG. 5: S-wave bottomonium T-matrices as a function of real (E_R) and imaginary (E_I) energies at zero center-of-mass momentum at various temperatures for a weak potential constrained by HQ free energies [19].

and a weakly coupled system, we exhibited the sensitivity of the quarkonium states to the underlying potential strength. Surprisingly, despite large collisional widths of the b-quarks in a strongly coupled QGP, the bottomonium states do not undergo a rapid melting, but continue to exist as broad states to much higher temperatures than expected from schematic criteria based on the energy uncertainty between their decay width and "binding energy". The latter is, after all, not well defined in the presence of broad spectral functions of the constituents. For example, the $\Upsilon(2S)$ state can persist up to a temperature of 0.7 GeV, with even higher temperatures for the $\Upsilon(1S)$. Elaborating the consequences of these findings for the phenomenology of heavy-ion collisions, in particular the quantitative sensitivity of observables to the persistence of hadronic states in the sQGP, will be an important objective for future transport studies. But the implications of our work go beyond the realm of quarkonia. The question of degrees of freedom in the QGP equation of state and the transition back into a hadronic medium are at the core of the physics of a strongly coupled quantum system which is driven by an interplay of large collisional widths and emerging composite states; our study has revealed that this interplay can lead to rather unexpected results.

Acknowledgments.— This work has been supported by the U.S. National Science Foundation under grant no. PHY-2209335, by the U.S. Department of Energy, Office of Science, Office of Nuclear Physics through contract No. DE-SC0012704 and the Topical Collaboration in Nuclear Theory on Heavy-Flavor Theory (HEFTY) for QCD Matter under award no. DE-SC0023547.

- E. Shuryak, Quark-gluon plasma, heavy ion collisions and hadrons (World Scientific, Singapore, 2024), ISBN 978-981-12-8234-8, 978-981-12-8236-2.
- [2] W. Busza, K. Rajagopal, and W. van der Schee, Ann. Rev. Nucl. Part. Sci. 68, 339 (2018), 1802.04801.
- [3] T. Matsui and H. Satz, Phys. Lett. B 178, 416 (1986).
- [4] E. Eichten, K. Gottfried, T. Kinoshita, K. D. Lane, and T.-M. Yan, Phys. Rev. D 21, 203 (1980).

- [5] G. S. Bali, Phys. Rept. 343, 1 (2001), hep-ph/0001312.
- [6] A. Andronic et al., Eur. Phys. J. A 60, 88 (2024), 2402.04366.
- [7] R. Rapp, D. Blaschke, and P. Crochet, Prog. Part. Nucl. Phys. 65, 209 (2010), 0807.2470.
- [8] P. Braun-Munzinger and J. Stachel, Landolt-Bornstein 23, 424 (2010), 0901.2500.
- [9] L. Kluberg and H. Satz (2010), 0901.3831.
- [10] A. Mocsy, P. Petreczky, and M. Strickland, Int. J. Mod. Phys. A 28, 1340012 (2013), 1302.2180.
- [11] Y. Liu, K. Zhou, and P. Zhuang, Int. J. Mod. Phys. E 24, 1530015 (2015).
- [12] D. Cabrera and R. Rapp, Phys. Rev. D 76, 114506 (2007), hep-ph/0611134.
- [13] Z. Tang, S. Mukherjee, P. Petreczky, and R. Rapp (2024), 2411.09132.
- [14] S. Navas et al. (Particle Data Group), Phys. Rev. D 110, 030001 (2024).
- [15] R. A. Briceno, J. J. Dudek, and R. D. Young, Rev. Mod. Phys. 90, 025001 (2018), 1706.06223.
- [16] F.-K. Guo, C. Hanhart, U.-G. Meißner, Q. Wang, Q. Zhao, and B.-S. Zou, Rev. Mod. Phys. 90, 015004 (2018), [Erratum: Rev.Mod.Phys. 94, 029901 (2022)], 1705.00141.
- [17] M. Albaladejo, J. M. Nieves, and L. Tolos, Phys. Rev. C 104, 035203 (2021), 2102.08589.
- [18] F. Riek and R. Rapp, Phys. Rev. C 82, 035201 (2010), 1005.0769.
- [19] S. Y. F. Liu and R. Rapp, Phys. Rev. C 97, 034918 (2018), 1711.03282.
- [20] E. Megias, E. Ruiz Arriola, and L. L. Salcedo, JHEP 01, 073 (2006), hep-ph/0505215.
- [21] A. Bazavov et al. (HotQCD), Phys. Rev. D 90, 094503 (2014), 1407.6387.
- [22] Z. Tang and R. Rapp, Phys. Rev. C 108, 044906 (2023), 2304.02060.
- [23] M. Laine, O. Philipsen, P. Romatschke, and M. Tassler, JHEP 03, 054 (2007), hep-ph/0611300.
- [24] Z. Tang, S. Mukherjee, P. Petreczky, and R. Rapp, Eur. Phys. J. A 60, 92 (2024), 2310.18864.
- [25] L. Roca, E. Oset, and J. Singh, Phys. Rev. D 72, 014002 (2005), hep-ph/0503273.
- [26] D. Gamermann, E. Oset, D. Strottman, and M. J. Vicente Vacas, Phys. Rev. D 76, 074016 (2007), hepph/0612179.
- [27] R. Larsen, S. Meinel, S. Mukherjee, and P. Petreczky, Phys. Rev. D 100, 074506 (2019), 1908.08437.